INSTANTANEOUS MASS TRANSFER MEASUREMENT AND ITS RELATION TO TURBULENCE STRUCTURES IN PIPE FLOW

Tong Tong

Department of Energy Engineering and Science
Graduate School of Engineering
Nagoya University
Furo-cho, Chikusa-ku, Nagoya, Japan 464-8601
ttgua1991@hotmail.com

Hironori Ito

Department of Energy Engineering and Science
Graduate School of Engineering
Nagoya University
Furo-cho, Chikusa-ku, Nagoya, Japan 464-8601
ito.hironori@h.mbox.nagoya-u.ac.jp

Takahiro Ito

Department of Energy Engineering and Science
Graduate School of Engineering
Nagoya University
Furo-cho, Chikusa-ku, Nagoya, Japan 464-8601
takaito@nucl.nagoya-u.ac.jp

Yoshiyuki Tsuji

Department of Energy Engineering and Science
Graduate School of Engineering
Nagoya University
Furo-cho, Chikusa-ku, Nagoya, Japan 464-8601
c42406a@nucc.cc.nagoya-u.ac.jp

ABSTRACT

In turbulent pipe flow, large-scale structures occur over a wide range of length and time scales, whose length is estimated to be of the order of 20R, where R is the pipe radius (Hutchins and Marusic, 2007) and may persist over long periods of time. Due to such large-scale events maintain a footprint in the near-wall region, some studies have revealed the relation between large-scale structure and shear stress (Hutchins and Marusic, 2007). However, since the mass transfer can be correlated with momentum by the analogy between both transport phenomena, we believe the large-scale events will also affect the mass transfer rate. In this study, we will focus on effects from large-scale structures on the mass transfer rate through a simultaneous measurement of mass transfer rate and velocity field.

INTRODUCTION

The flow fluctuations near the wall are paramount in many practical applications one of them is transport phenomena, including momentum and mass transfer. Up to now, there are many studies about the relation between shear stress fluctuation and turbulence structures. However, since the mass transfer can be correlated with shear stress by the analogy between both transport phenomena, attempt to understand how turbulence structure affect close to the wall for mass transfer, the physical mechanism by which turbulence structures augment mass transfer is a fundamental problem of turbulent flows.

In turbulent flow, there exists a regime of very long meandering positive and negative streamwise velocity fluctuations in log-region, however, in the near wall region, there exists corresponding streamwise velocity fluctuations. Such large-scale events in the near wall region is called “a footprint of the large-scale structure” from the log-region (Hutchins and Marusic, 2007). Therefore, in the near wall region, the mass transfer rate must be affected by such large-scale structures.

In this study, we want to clarify the relation between large-scale structure and mass transfer rate from experiment. Firstly, we will check the large-scale structure and its footprint in the near wall region, and then we independently analyze the mass transfer fluctuation, finally we do the simultaneous measurement to detect how large scale structure affect the mass transfer fluctuation. And what kinds of large-scale properties will enhance the mass transfer rate.

EXPERIMENTAL TECHNIQUE

Figure 1 shows the test section, which housed the electrodes. Among the straight pipe, eight working cathodes are located along spanwise direction, the degree between each electrode is 8°. Besides, other eight cathodes are located along the streamwise direction, the distance between each other is 0.2D, where D is the pipe’s inner diameter. All working cathodes are constructed by inserting a cylindrical gold wire with a diameter of 1 mm into the pipe wall. The counter and reference electrodes are located far away from the working electrodes in the downstream region, respectively. The counter electrode (anode) is a nickel circular ring with a thickness of 5 mm. The relatively large size of the counter electrode (anode), compared with that of the cathodes, is selected to ensure that the current flowing into the circuit is controlled by reactions at the cathode surface. All electrodes are mounted flush with the pipe wall, therefore, no abrupt change of the hydrodynamic conditions occurred in the connection region between the electrodes and the pipe wall.

We first used a potentiostat to measure the current–voltage relationship at each local working cathode to obtain the range of voltage in which the current is mass transfer rate controlled and the profile of the mass transfer rate. The velocity field is measured by a stereo-PIV system, like figure 2, which consisted of two digital high-speed complementary metal-oxide semiconductor (CMOS) cameras (High-SpeedStar 4G), an Nd: YLF laser, a high-speed controller, and a desktop personal computer for analyzing the PIV data. Davis 8.1 commercial PIV software is used to operate the hardware of the PIV system and to calculate the velocity fields.

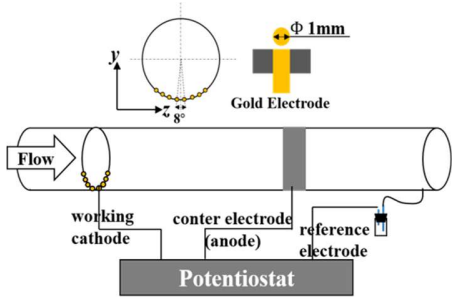

Figure 1. Test section for mass transfer measurement.

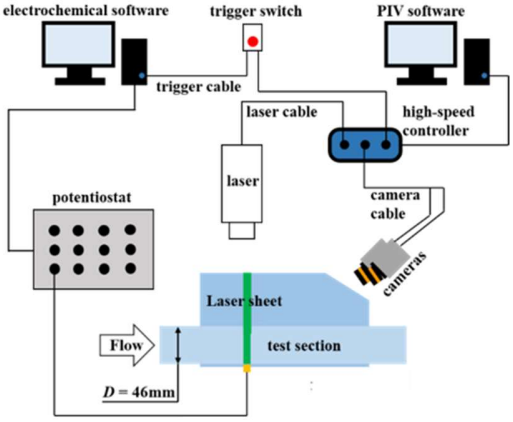

Figure 2 Schematic view of PIV system.

The test solution is an equilibrium mixture of potassium ferricyanide ($K_3Fe(CN)_6$) and potassium ferrocyanide ($K_4Fe(CN)_6$) with potassium sulfate (K_2SO_4) as the supporting electrolyte, the ions of which are not involved in the electrode reactions. De-ionized water and high-purity chemicals (analytical reagents) are used to compose the 70 L of solution. The temperature of the electrolyte is maintained at 20℃ throughout the measurement process. Precautions are taken to avoid contamination of electrolyte and electrode surfaces. More specifically, the solution is protected from exposure to daylight as much as possible and is deaerated and kept under a blanket of inert nitrogen gas. Previous studies have detailed the mass transfer measurement and principles of the LDCT (Mizushina, 1971).

RESULTS AND DISCUSSION

1. Streamwise Velocity Distribution

We check the feasibility of our data by the mean velocity profile, comparing with the data of direct numerical simulation (DNS). As shown in figure 3, streamwise mean velocity is plotted against the distance from the wall. Both are almost overlap with each other especially in the log-region.

We also plot the contour of instantaneous streamwise velocity over constant radial surface at $y^+ = 111$. Figure 4 exhibits the streak structures of positive high-fluctuation elongated and flanked by either side of negative high-fluctuation structures within very narrow azimuthal dimension. Such consistent structure with long period time is the so-called large-scale structure. Here, the vertical axis s is the length along pipe surface.

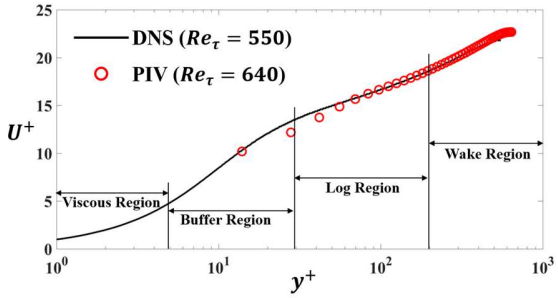

Figure 3 Mean velocity profile of PIV and DNS. Re_τ is Reynolds number based on friction velocity and pipe radius. Solid line is the data of DNS by Khoury et al. (2013) and open circles are PIV result.

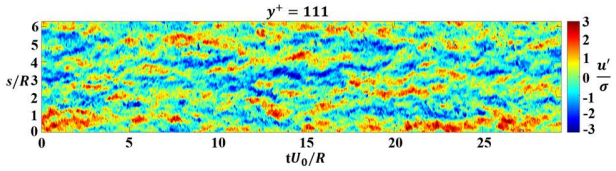

Figure 4 Contour of instantaneous streamwise velocity fluctuation over the radial surface at $y^+ = 111$.

2. Mass Transfer Fluctuation in Azimuthal Direction

Figure 5 shows the contour of instantaneous mass transfer fluctuation over the azimuthal direction in cylindrical system. s is the circumference at some constant radial point from the wall. It is obvious that along the spanwise direction, positive mass transfer fluctuation flanks on either side of the negative mass transfer fluctuation, which show the similar fluctuation tendency with the streamwise velocity field. Therefore, we consider such kind of mass transfer fluctuation is related to the streamwise velocity fluctuation.

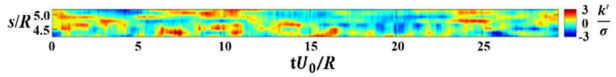

Figure 5 Contour of instantaneous mass transfer fluctuation on the wall.

3. Relation Between Streamwise Velocity Fluctuation and Mass Transfer Fluctuation

Figure 6 shows the comparison among the mass transfer fluctuation and streamwise velocity fluctuation in different regions. In the region, which is close to the wall ($y^+ = 14$), the velocity fluctuation shows almost same tendency with the mass transfer rate. The positive fluctuation of velocity results in the positive mass transfer fluctuation. However, you can find the velocity in log-region ($y^+ = 111$) also shows the similar tendency with the mass transfer fluctuation.

It seems that the velocity fluctuation from the log-region also has some effect on the mass transfer rate. This is called the footprint (Hutchins and Marusic, 2007). We consider that the large-scale structure from the log-region will enhance the mass transfer rate.

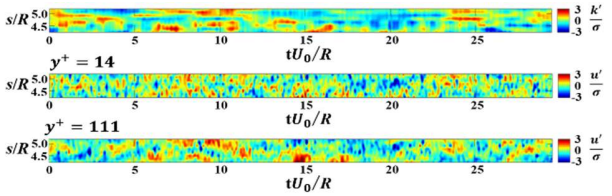

Figure 6 Contour of mass transfer fluctuation and streamwise velocity fluctuation.

In order to quantitatively characterize the velocity fluctuation and mass transfer fluctuation, the coarse-grained structures are studied instead of the original flow field. According to figure 6, we removed some parts of data, only preserve the parts, whose fluctuation is larger than one time of their standard deviation, as well as one time smaller than negative standard deviation.

$$u_I = \begin{cases} 1: & u' \geq \sigma \\ 0: & -\sigma < u' < \sigma \\ -1: & u' \leq -\sigma \end{cases} \quad (1)$$

$$k_I = \begin{cases} 1: & k' \geq \sigma \\ 0: & -\sigma < k' < \sigma \\ -1: & k' \leq -\sigma \end{cases} \quad (2)$$

We set the time-lag as Δt, and define the correlation coefficient as

$$C_{ku} = \frac{1}{T}\int_0^T u_I(t)k_I(t+\Delta t)dt \quad (3)$$

where u' is the streamwise velocity fluctuation, k' is the mass transfer fluctuation, σ is the standard deviation for each quantity, T is the sampling total time.

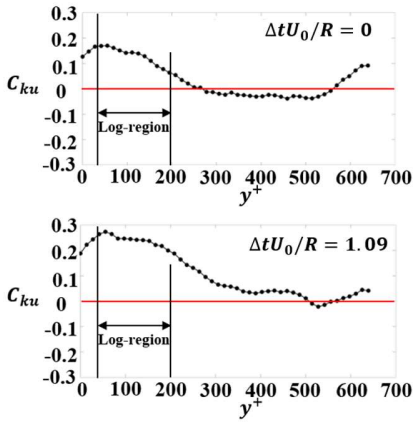

Figure 7 Correlation between mass transfer rate and velocity fluctuation along the direction from wall to pipe centre.

Figure 7 shows the time correlation between mass transfer rate and velocity fluctuation along the direction from wall to pipe centre. When $\Delta t = 0$, we can find that the correlation coefficient increases to the peak in the log-region. Then gradually decreases outward. Besides, there also exists some part that is negative correlated. When we slight increase the time-lag as $\Delta tU_0/R = 1.09$, the overall locations show positive correlation. And the peak value of correlation coefficient becomes larger in the log-region. From this result, we believe there exists some time-lag between the large-scale structure attachment and mass transfer enhancement. And the footprint affects the mass transfer late.

In order to clarify the reason of the existence of time lag, the contour of two-dimensional correlation coefficient is plotted as shown in figure 8, horizontal axis Δx^+ is the flow direction, vertical axis y^+ is the distance against to the wall. From figure 8, high correlation region locates inside log-region and near wall region. And this high-correlation region is inclined toward the downstream.

$$\Delta x = u_c(y)\times\Delta t \quad (4)$$

$$\Delta x^+ = \Delta x u_\tau/\nu \quad (5)$$

$$y^+ = y u_\tau/\nu \quad (6)$$

where, $u_c(y)$ is local mean velocity, Δt is time lag.

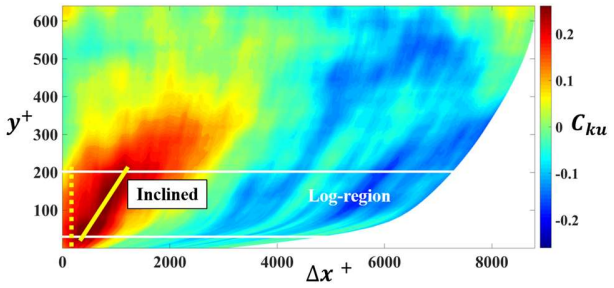

Figure 8 Two-dimensional contour of the correlation coefficient C_{ku}. Thresholds of both coarse-grained velocity and mass transfer are one time of their standard deviations.

The thresholds of both velocity fluctuation u' and mass transfer fluctuation k' are set as one time of their standard deviation respectively, in the above coarse-grained analysis. However, up to now, there is no unified standard of the threshold for the coarse-grained analysis. Here, we fixed one position in the log-region as $\Delta x^+ = 752$ and $y^+ = 125$ in figure 9. Then pick up the coarse-grained structures by the following equations,

$$u_I = \begin{cases} 1: & u' \geq A\sigma \\ 0: & -A\sigma < u' < A\sigma \\ -1: & u' \leq -A\sigma \end{cases} \quad (7)$$

$$k_I = \begin{cases} 1: & k' \geq B \\ 0: & -B\sigma < k' < B \\ -1: & k' \leq -B\sigma \end{cases} \quad (8)$$

where A=0.1, 0.2, ··· 2, B=0.1, 0.2, ··· 2.

We calculate the correlation coefficient between coarse-grained velocity fluctuation and mass transfer fluctuation at the fixed position ($\Delta x^+ = 752$ and $y^+ = 125$), with different thresholds of A and B, region from 0.1 to 2.0. Figure 9 shows the contour of correlation coefficient at constant position. The peak value in figure 9 locates in the position where A=0.7 and B=0.5, which means velocity and mass transfer rate are not linear correlated in the coarse-grained structures. Figure 10 shows the comparison of C_{ku} distribution between two coarse-grained thresholds. From figure 10, not only the large-scale structures ($u' \geq \sigma, u' \leq -\sigma$), the relatively small-scale structures will also contribute to the mass transfer fluctuation.

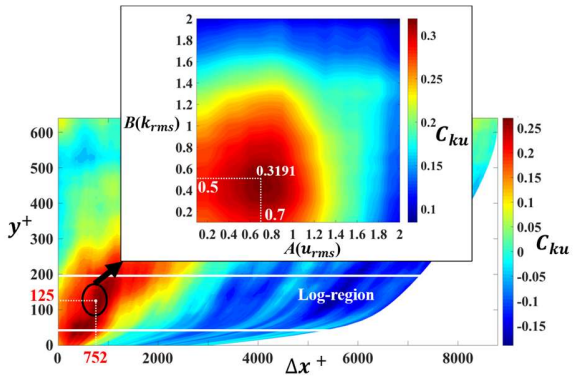

Figure 9 Contour of C_{ku} at position of $\Delta x^+ = 752$ and $y^+ = 125$, with different thresholds of coarse-grained structure.

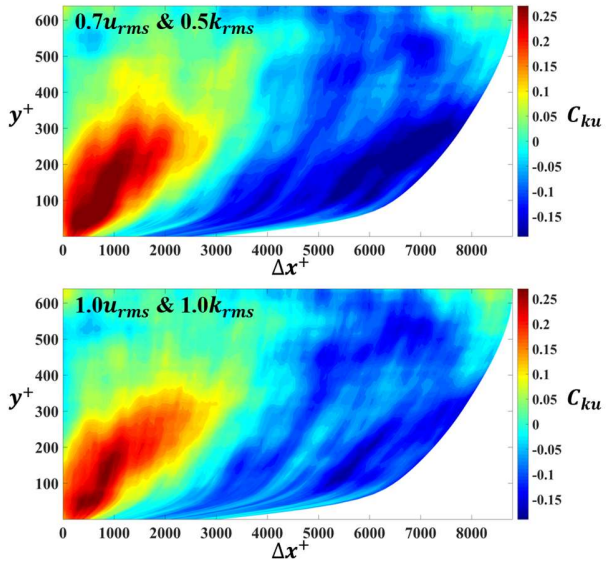

Figure 10 Two-dimensional contour of the correlation coefficient C_{ku}. In upper one, thresholds of coarse-grained velocity is $0.7u_{rms}$ and mass transfer is $0.5k_{rms}$. in below one, thresholds of coarse-grained velocity is $1.0u_{rms}$ and mass transfer is $1.0k_{rms}$.

Therefore, the model of large-scale structures how they affect the mass transfer rate at wall is considered, as shown in figure 11. The large-scale structures are carried by local mean velocity, outer region moves faster than inner region. Besides, large-scale structure has footprint on the wall, however, its effect is not perpendicular to the wall but inclined toward the downstream. Thus, these will make a time-lag between velocity and mass transfer rate.

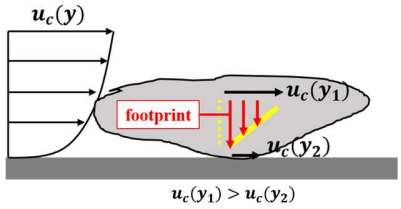

Figure 11 Model of large-scale structure affecting the wall.

4. Large-scale Motion from View of Mass Transfer Rate

To detect the large-scale motion along both spanwise and streamwise direction, two cases, as shown in figure 12, are discussed in order to predict the large-scale motion from mass transfer rate. We calculate the two-point correlation of mass transfer rate between different positions for analyzing the large-scale motion. Case1 is for checking the spanwise movement, case2 is for checking the streamwise movement.

$$R_{mn}(\tau) = \frac{\overline{k_m(t)k_n(t+\tau)}}{\sqrt{\overline{k_m(t)^2}}\sqrt{\overline{k_n(t)^2}}} \quad m,n = 1, 2, \cdots 8 \qquad (9)$$

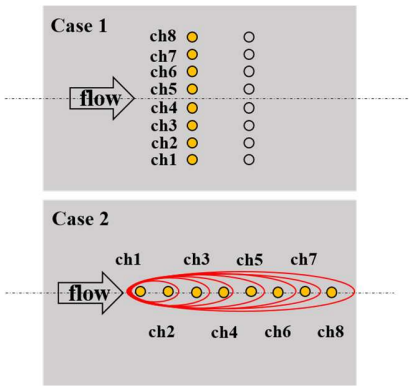

Figure 12 Two cases.

Firstly, spanwise motion of Case1 is checked by the time correlation coefficients of R_{34}, R_{45}, R_{56} and R_{67}. From figure 13, all of the peaks almost overlap with each other and around time lag $\tau = 0$. From figure 13, it looks that the motions of large-scale structures along spanwise direction osillate independently between each other. The same results we can also found from the space correlation of mass transfer rate between each spanwise positions, as shown in figure 14. The solide line is the space correlation of velocity fluctuation R_{uu} at $y^+ = 56$, along spanwise direction, the

dark points are space correlation of mass transfer fluctuation R_{kk}. We can find the correlation coefficient suddenly decreases around zero, which confirm that the motion of large-scale structure are independent among its neigbhours. The width of large-scale structure is about 0.3R, where R is pipe radius.

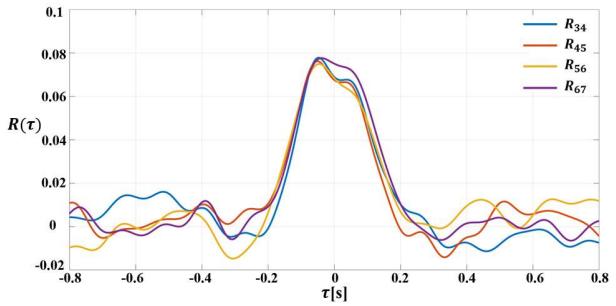

Figure 13 Two-point correlation along spanwise direction of Case1.

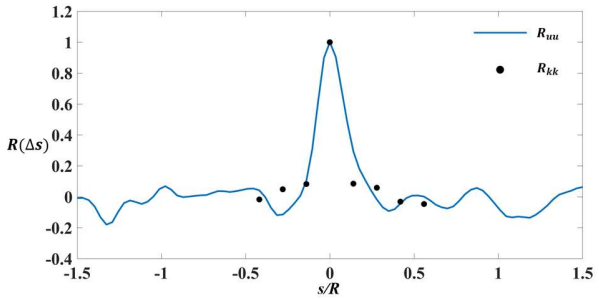

Figure 14 Space correlation along spanwise direction of Case1. Solid line is the space correlation of streamwise velocity at $y^+ = 56$. Dark point is the space correlation of mass transfer rate.

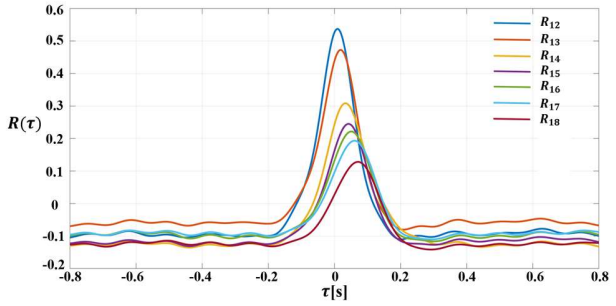

Figure 15 Two-point correlation along streamwise direction of Case2.

From case 2, calculate the correlation between ch1 and all other channels, along streamwise direction. The time lags of the peaks, as shown in figure 15, increase far from p1 along the downstream, as well as the maximum correlation coefficient decrease along the downstream (figure 16), which means there are no oscillations and shape deformation along the downstream. Therefore, along the streamwise direction, the shape of large-scale structure keeps almost constant, and such structure gradually moves to the downstream without any ocsillations.

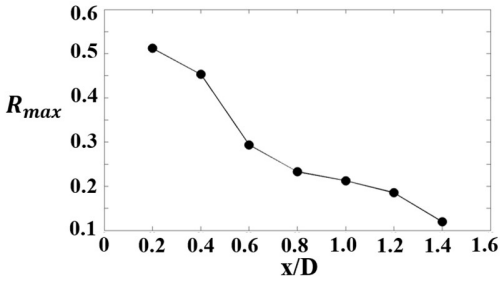

Figure 16 Peak value of correlation coefficient along downstream.

CONCLUSION

From the simultaneous measurement of velocity and mass transfer fluctuation in the pipe flow, we characterized the large-scale structures by way of coarse-grained analysis. The results are summarized as follows:

(1) Large-scale structures have a significant effect on the mass transfer rate at the wall. The correlation coefficient is at almost 30% in the log-region.

(2) There is a time-lag when the velocity fluctuation affect the wall. The space correlation of C_{ku} contour shows the inclined structures toward the downstream. Therefore, the footprint might occur with time-lag.

Based on these results, we hope the mass transfer rate can be enhanced by controlling the large-scale structures.

From the view of mass transfer rate, we imaged the large-scale motion. The spanwise motion of large-scale structures near the wall is independent among their neighbors. In the streamwise direction, the large-scale shape almost keeps constant, and it moves gradually to the downstream with out any oscillation. With the large-scale motion, the mass transfer rate will be enhanced with the same tendency.

REFERENCES

Hutchins N, Marusic I., 2007, " Evidence of Very Long Meandering Features in the Logarithmic Region of Turbulent Boundary Layers ", *Journal of Fluid Mechanics*, Vol. 579, pp. 1-28.

Mizushina, T., 1971, " The electrochemical method in transport phenomena," *Advances in Heat Transfer*, Vol. 7, pp. 87-161.

El Khoury, G. K., Schlatter, P., Noorani, A., Fischer, P. F., Brethouwer, G., & Johansson, A. V., 2013, " Direct numerical simulation of turbulent pipe flow at moderately high Reynolds numbers", *Flow, turbulence and combustion*, Vol. 91(3), pp. 475-495.